

ADVANCED FUNCTIONAL MATERIALS

Supporting Information

for *Adv. Funct. Mater.*, DOI: 10.1002/adfm.201102393

Photoconductive Hybrid Films via Directional Self-Assembly
of C₆₀ on Aligned Carbon Nanotubes

*Eric R. Meshot, Keval D. Patel, Sameh Tawfik, K. Anne
Juggernaut, Mostafa Bedewy, Eric A. Verploegen, Michaël
F. L. De Volder, and A. John Hart**

For

**Photoconductive hybrid films via directional self-assembly of C₆₀ on aligned carbon
nanotubes**

**Eric R. Meshot,[†] Keval D. Patel,[†] Sameh Tawfick,[†] K. Anne Juggernaut,^{†‡} Mostafa
Bedewy,[†] Eric A. Verploegen,[‡] Michaël F. L. De Volder,^{§¹} and A. John Hart^{†*}**

[†]*Department of Mechanical Engineering, University of Michigan, 2350 Hayward Street, Ann
Arbor, Michigan 48109, USA.*

[‡]*Macromolecular Science and Engineering Research Center, University of Michigan, 2300
Hayward Street, Ann Arbor, MI 48109 USA.*

[‡]*Stanford Synchrotron Radiation Lightsource, SLAC National Accelerator Laboratory 2575
Sand Hill Road, Menlo Park, CA 94025.*

[§]*IMEC, Kapeldreef 75, 3001 Heverlee, Belgium,*

¹*Department of Mechanical Engineering, KULeuven, Celestijnenlaan 300B, 3001, Leuven,
Belgium,*

*Address correspondence to ajohnh@umich.edu

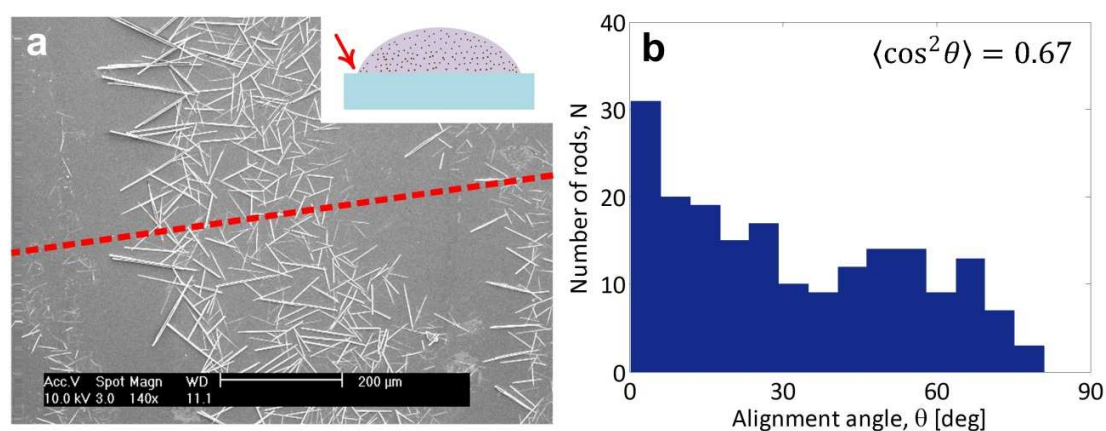


Figure S1. (a) SEM image of C₆₀ crystals grown by drop-casting C₆₀/*m*-xylene on Si, taken in a region where the solvent pinned^[1] to the substrate during drying. Inset schematic shows the location where the droplet pinned to the Si. The red dashed line represents the estimated radial direction of this drying ring and serves as the axis from which we measure the orientation angle of the C₆₀ rods. The results of these measurements are in the histogram (b) with $\langle \cos^2 \theta \rangle = 0.67$.

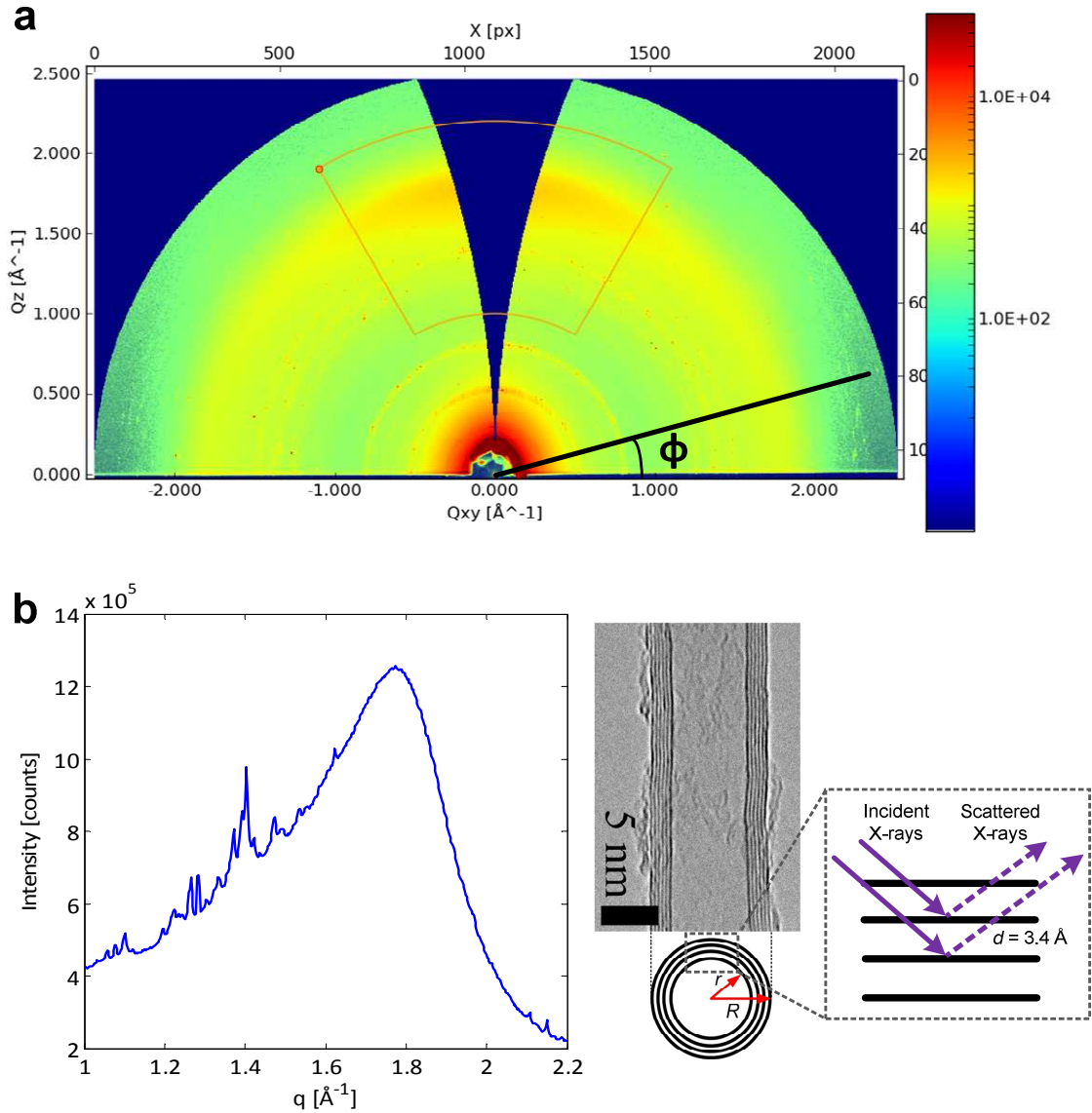


Figure S2. (a) Representative 2D scattering image for C_{60} crystals on laterally oriented CNTs (X-ray beam parallel to CNT direction). The plots of intensity versus scattering vector q in Fig. 3b were obtained by integrating the intensity in the 2D image above about the azimuthal angle ϕ [$1^\circ, 179^\circ$]. (b) Azimuthally integrated intensity of the sector outlined in a) showing the

diffraction peak from the CNT wall spacing (peak at 1.78 \AA^{-1} corresponds to d -spacing of 3.53 \AA , which agrees with the interplanar spacing of graphite 3.4 \AA).^[2]

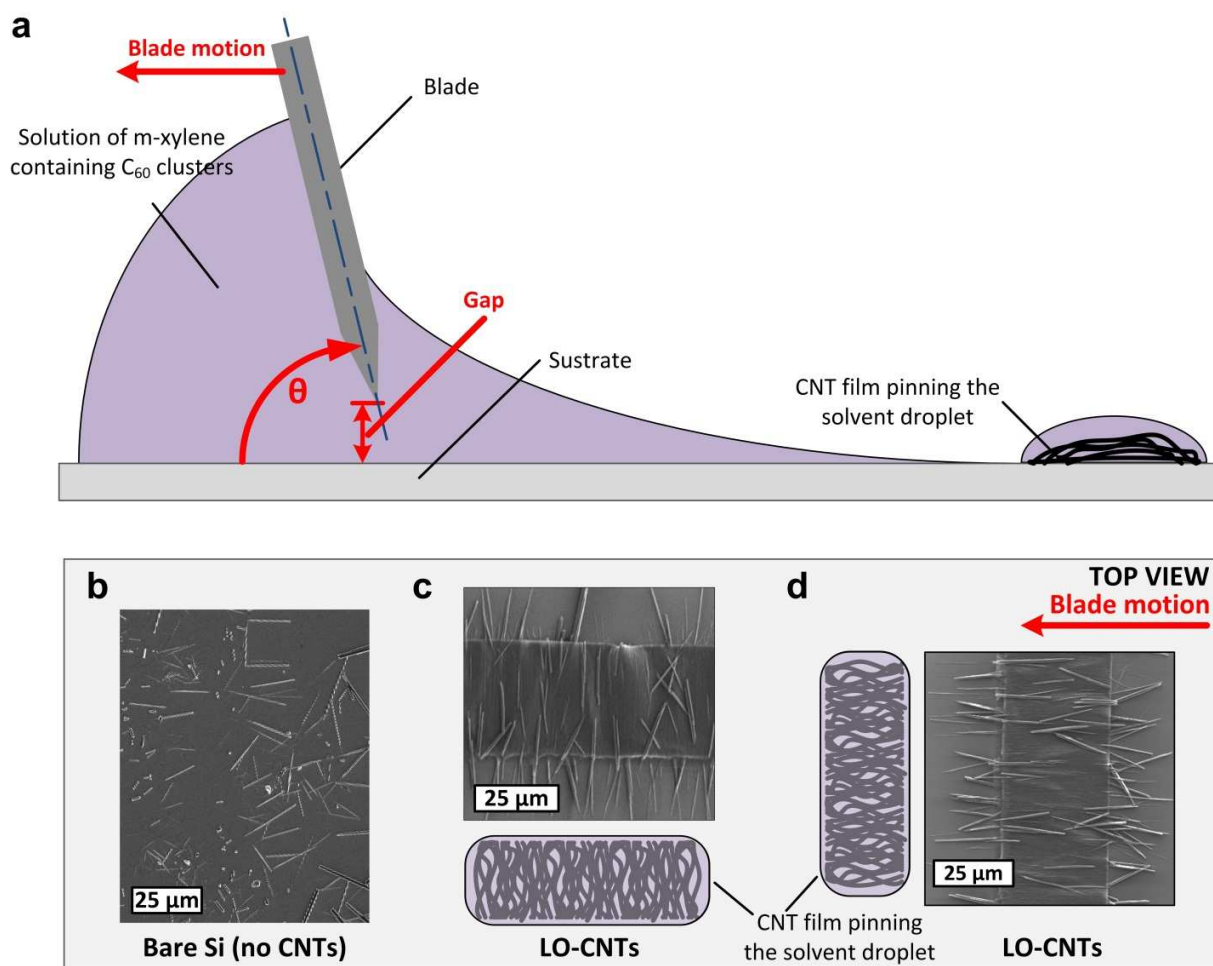


Figure S3. (a) Using a blade to guide the solvent's meniscus is a way to directionally control evaporation,^[3] and (b) on bare Si, we see evidence of poor alignment with the direction of the blade's motion. Schematic representation of the blade casting process shows pinning of a droplet of C_{60} dispersion to the CNT film regardless of the relative direction of blade motion (always to the left as indicated by the red arrow): a) side view and top views where the blade motion is (c) perpendicular and d) parallel to the CNT direction. Instead of drop-casting, the C_{60}

dispersion is drawn across the CNT film with a 10- μm gap between the blade and the substrate, and the blade is drawn using a motorized stage at a speed of 10 $\mu\text{m sec}^{-1}$.

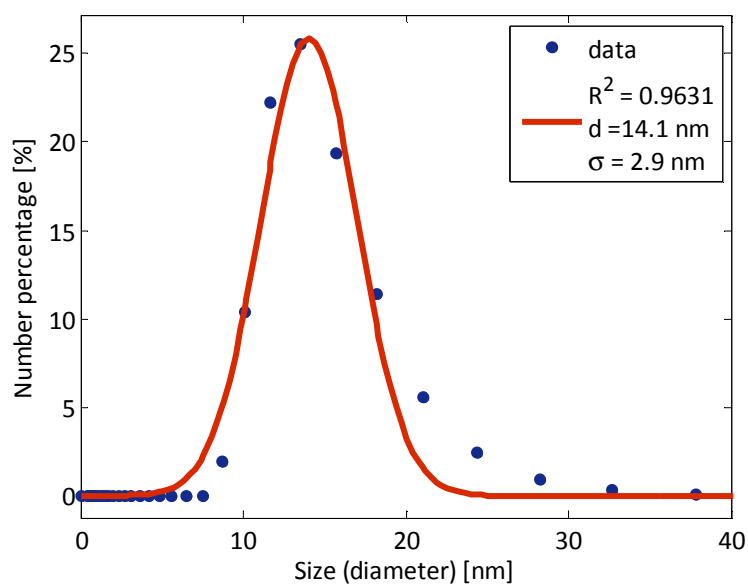


Figure S4. Dynamic Light Scattering measurement of C_{60} dispersed in *m*-xylene (1 mg/mL) after 30 minutes of ultrasonication. The number of C_{60} in each cluster in solution is calculated from the measured average cluster size and by assuming hexagonal packing with unit cell dimensions that were measured by X-ray diffraction. The mean cluster diameter is equal to $14.1 \pm 2.9 \text{ nm}$, representing $\approx 300\text{-}1100 \text{ C}_{60}$ per cluster is.

References

- [1] R. D. Deegan, O. Bakajin, T. F. Dupont, G. Huber, S. R. Nagel, T. A. Witten, *Nature* **1997**, *389*, 827-829.
- [2] H. Furuta, T. Kawaharamura, M. Furuta, K. Kawabata, T. Hirao, T. Komukai, K. Yoshihara, Y. Shimomoto, T. Oguchi, *3*.
- [3] L. Malaquin, T. Kraus, H. Schmid, E. Delamarche, H. Wolf, *Langmuir* **2007**, *23*, 11513-11521.